PROCEEDINGS OF SCIENCE

Learning about Dark Matter from the Stars

Joachim Kopp*
Theoretical Physics Department, CERN, Geneva, Switzerland
and PRISMA Cluster of Excellence, University of Mainz, Germany
E-mail: jkopp@cern.ch

We discuss several novel astrophysical methods for elucidating the nature and the distribution of dark matter in the Universe. First, we argue that subhalos of the Milky Way's dark matter halo traveling through the disk will leave a characteristic imprint in the motion of nearby stars. These "stellar wakes" can be probed using precise astrometric data, for instance from Gaia. In the second part of the talk, we illustrate how gravitational lensing and pulsar timing can constrain compact dark matter objects such as primordial black holes or axion mini-clusters. Finally, we comment on the prospects of probing the dark sector using gravitational wave signals form neutron star mergers.

Neutrino Oscillation Workshop (NOW2018)
9 - 16 September, 2018
Rosa Marina (Ostuni, Brindisi, Italy)

*Speaker.

PoS(NOW2018)081

1. Introduction

Astroparticle physics is in the fortunate situation that an abundance of new data is available to help us unravel some of the most profound mysteries of the Universe. Precise astrometric measurements from the Gaia satellite are transforming our understanding of the Milky Way. Data from the Fermi mission is offering us unprecedented views of the gamma ray sky. And the discoveries by the LIGO and Virgo gravitational wave observatories have set the foundations for a whole new branch of astronomy. In this talk, we explore several novel ways in which these data sets can teach us about dark matter (DM). In section 2, we will illustrate how Gaia could probe perturbations to the phase space distribution of stars caused by the passage of dark matter subhalos. Afterwards, in section 3, we will show that gamma ray bursts (GRBs) observed by Fermi can be gravitationally lensed by compact DM objects such as primordial black holes (PBHs) along the line of sight. We will in particular explore the regime of femtolensing, where interference between multiple images of the source leads to characteristic features in its energy spectrum. Finally. in section 4, we will explore the possibility that the gravitational wave signals from binary neutron star mergers may be affected by the dynamics of the DM particles contained within. Specifically, we will discuss the impact of long-range DM self-interactions on the inspiral.

2. Gaia: Stellar Wakes

Simulations of galaxy formation predict that the Milky Way's dark matter halo is not smooth, but rather features substructures across many order of magnitude in mass [1]. The most massive among these substructures ($\gtrsim 10^9 M_\odot$) contain enough baryons to form stars and are therefore visible as dwarf galaxies. Smaller substructures, on the other hand, have remained elusive so far. As has been shown in ref. [2], this may change with the data collected by Gaia.

In fig. 1, we show that the passage of a DM subhalo, with the parameters given in the caption, affects the stellar phase space distribution, leaving characteristic "wakes". The structure of these wakes can be obtained semi-analytically by solving the Boltzmann equation for the 6d phase space distribution $f(\vec{x},\vec{v},t)$. The Boltzmann equation reads

$$\frac{\partial f}{\partial t} + \vec{v}\cdot\vec{\nabla}_x f - \vec{\nabla}_x\Phi\cdot\vec{\nabla}_v f = 0\,. \tag{2.1}$$

Here, $\Phi(\vec{x})$ is the gravitational potential of the DM subhalo. Since stellar wakes are a weak effect, a perturbative treatment is justified. We therefore write

$$f(\vec{x},\vec{v},t) = f_0(\vec{v}) + f_1(\vec{x},\vec{v})\,, \tag{2.2}$$

where $f_0(\vec{v})$ is the unperturbed phase space distribution (approximately isothermal and spatially homogeneous), and $f_1(\vec{x},\vec{v},t)$ is the perturbation. To first order in $f_1(\vec{x},\vec{v})$, eq. (2.1) is solved by [4]

$$f_1(\vec{x},\vec{v}) = \int_0^\infty \frac{du}{u^2}\,\vec{\nabla}_y\Phi(\vec{y})\cdot\vec{\nabla}_v f_0(\vec{v})\Big|_{\vec{y}=\vec{x}-\vec{v}/u}\,. \tag{2.3}$$

We define a likelihood function

$$p(d|\boldsymbol{\theta}) = e^{-N_{\rm star}(\boldsymbol{\theta})}\prod_{k=1}^{\bar{N}_{\rm star}} f(\vec{x}_k,\vec{v}_k)(\boldsymbol{\theta})\,, \tag{2.4}$$

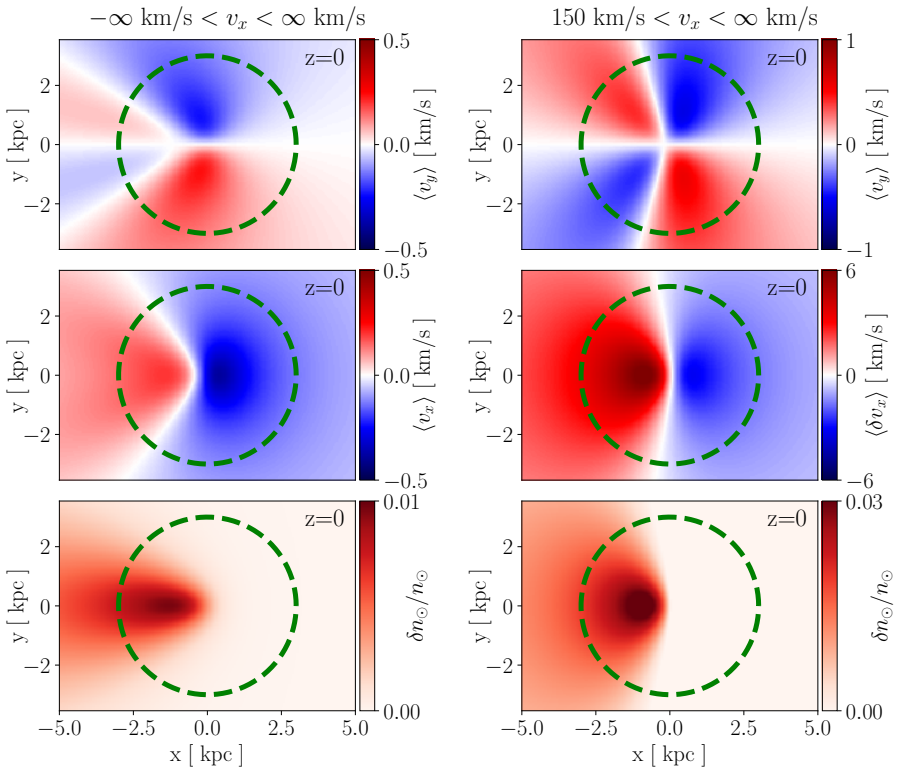

Figure 1: *Left:* Effect of a passing DM subhalo (located at the origin and traveling in the positive x-direction) on the phase space distribution of stars. We assume a subhalo mass of $2 \times 10^7 M_\odot$, a Plummer sphere density profile [3] with scale radius $r_s = 0.72$ kpc, and a velocity of 200 km/sec. The initial velocity distribution of the stars is assumed to have Maxwell–Boltzmann shape ($f_0(\vec{v}) \propto \exp(-v^2/v_0^2)$, with $v_0 = 100$ km/sec). In the top and middle panels, we show the average deviation of the in-plane velocities, while the bottom panels show the change in stellar density. *Right:* same as left, but including only stars with $v_x > 150$ km/sec (comoving with the subhalo).

where d refers to the data, $\boldsymbol{\theta}$ denotes the set of model parameters (position, velocity, mass, and density profile of the subhalo, properties of the background distribution of stars), and N_{star} is the total number of stars in the region of interest (ROI). We will be most interested in constraining the subhalo mass M_{sh}. For this purpose, we define the profile likelihood

$$\lambda(M_{\text{sh}}) = 2\left[\max_{\boldsymbol{\theta}_{\text{nuis}}} \log p(d|\mathscr{M}, \boldsymbol{\theta}) - \max_{\boldsymbol{\theta}} \log p(d|\mathscr{M}, \boldsymbol{\theta})\right], \tag{2.5}$$

where $\boldsymbol{\theta}_{\text{nuis}}$ refers to all model parameters other than M_{sh}.

In fig. 2, we show the behavior of $\lambda(M_{\text{sh}})$, obtained from N-body simulations. We see that the presence of a $2 \times 10^7 M_\odot$ subhalo can be easily identified at high significance $> 3\sigma$ ($\lambda(M_{\text{sh}}) > 9$). In the absence of a subhalo, it should be possible to set a 95% CL limit on the order of $M_{\text{sh}} \lesssim 10^7 M_\odot$, corresponding to $\lambda(M_{\text{sh}}) = -2.71$.

3. Fermi: Femtolensing of Gamma Ray Bursts

We now turn our attention to DM structures much more compact than the subhalos discussed

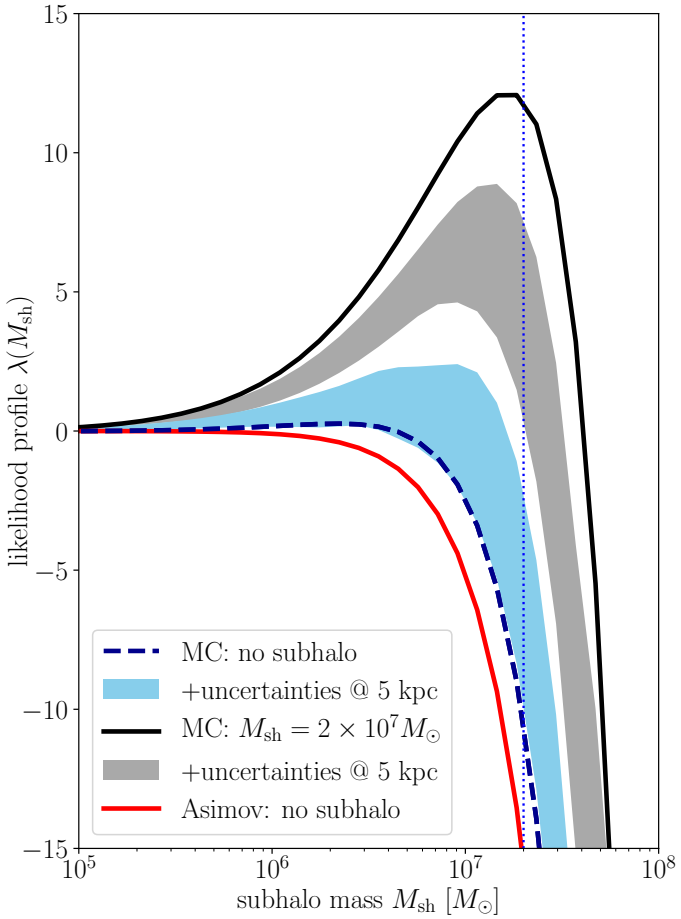

Figure 2: Statistical sensitivity to stellar wakes as a function of the subhalo mass. We show how the profile likelihood (defined in eq. (2.5)) varies as a function of the assumed subhalo mass if the data contains no subhalo (blue dashed line) and if there is a subhalo with the same parameters as in fig. 1 (solid black line). The blue and gray bands indicate the highly asymmetric 1σ uncertainties (stellar position, distance, and velocity uncertainties, subhalo direction). These sensitivity estimates are obtained from an N-body simulations, assuming a stellar density of 5×10^3 kpc^{-3} and using an ROI 6 kpc in diameter (green circle in fig. 1). They agree very well with an analytical analysis based on an Asimov data set (red solid line).

in section 2. In particular, we will explore constraints on PBHs based on femtolensing of GRBs [5, 6]. The term femtolensing refers to observations of gravitational lensing in which the multiple images of an astrophysical source cannot be spatially resolved, but interference patterns are observable in the source energy spectrum. This happens when the travel distances corresponding to different geodesics connecting the source to the observer differ by not more than several photon wave lengths. The following discussion is based on ref. [7].

GRBs are typically observed at keV–MeV energies (wave length 10^{-10}–10^{-7} cm), so femtolensing is expected to be most pronounced for lens masses between 10^{-17} and $10^{-14} M_\odot$ [6, 7]. The corresponding modulation of the signal spectrum is illustrated in fig. 3 for both idealized point-like sources *(left)* and more realistic extended sources *(right)*. Interference fringes are visible, but

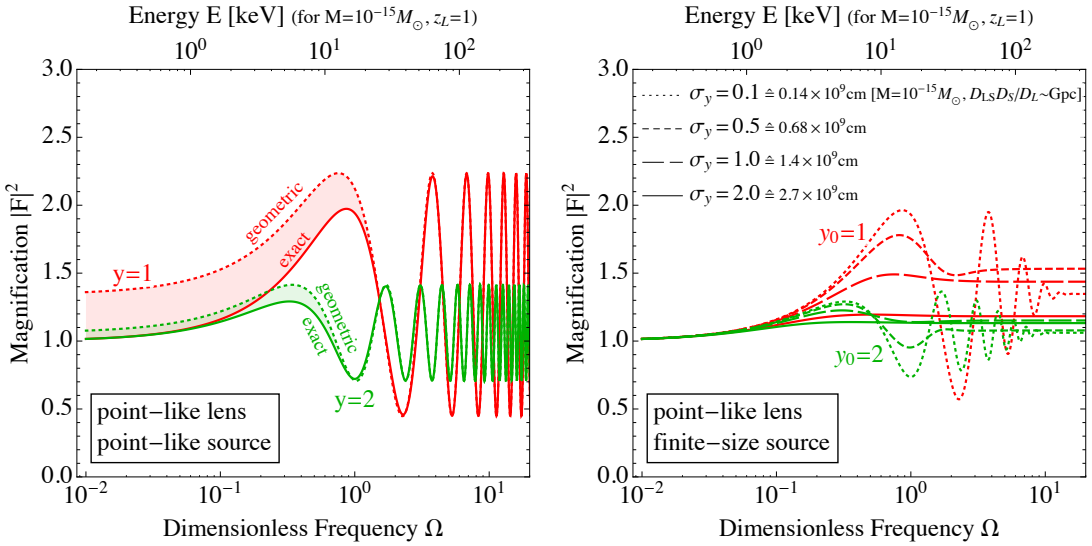

Figure 3: *Left:* Modulation of a GRB energy spectrum due to femtolensing for point-like source and point-like lens. Red curves correspond to a lens close to the (unperturbed) line of sight to the source, while green curves are for a lens somewhat further away from the line of sight. Dashed curves are for the geometric optics approximation, while solid curves take into account wave optics corrections. *Right:* Modulation for spatially extended sources of different diameters.

their magnitude is much smaller for extended sources. It also strongly depends on the angular distance between the lens and the would-be line of sight. This angular distance is quantified by a parameter $y \equiv \beta/\theta_E$, where β is the angle under which the source would be observed relative to the lens if there was no lensing, and θ_E is the Einstein angle. The latter gives the typical (angular) distance at which lensed photons pass the lens and can be written as

$$\theta_E \equiv \left(\frac{4GM}{c^2}\frac{D_{LS}}{D_S D_L}\right)^{1/2}. \tag{3.1}$$

Here, G is Newton's constant, M is the lens mass, c is the speed of light and D_{LS}, D_S, D_L are the distances between the lens and source, observer and source, and observer and lens, respectively.

Figure 3 illustrates that interference fringes can only be observed if the source is small ($\lesssim 10^9$ cm) and the lens if close to the line of sight. Moreover, by comparing the dotted and solid curves in the left panel of fig. 3, we also note that femtolensing becomes weaker when wave optics effects are taken into account. In a wave optics treatment, the observed signal is computed by solving the Fresnel integral [8]

$$F(\vec{y};\omega) \propto \int d^2\vec{x}\, e^{i\omega\Delta t(\vec{x},\vec{y})}, \tag{3.2}$$

which takes into account that the observer receives photons from any point $\vec{x}$ in the lens plane. $\vec{y}$ the location of the source, and both $\vec{x}$ and $\vec{y}$ are normalized to θ_E. ω is the photon angular frequency, and the time delay for a photon passing through coordinates $\vec{x}$ on the lens plane is [9]

$$\Delta t = \frac{1}{c}\frac{D_L D_S}{D_{LS}}(1+z_L)\left(\frac{|\vec{\theta}-\vec{\beta}|^2}{2} - \psi(\vec{\theta})\right), \tag{3.3}$$

where z_L is the redshift of the lens, $\vec{\beta} = \vec{y}\,\theta_E$ and $\vec{\theta} = \vec{x}\,\theta_E$ are the angular location of the source in the absence of lensing and the viewing angle of the images, respectively, and $\psi(\vec{\theta})$ is the lensing potential. For a point-like lens, it is given by $\psi(|\vec{\theta}|) = \theta_E^2 \log|\vec{\theta}|$. The geometric optics limit is obtained from a saddle point approximation to eq. (3.2).

In view of fig. 3, we conclude that, for realistic GRB sources with a diameter $> 10^9$ cm [10, 11], it will be extremely challenging to observe femtolensing. Therefore, previously claimed limits on PBHs based on this effect [6] are invalid because they were based on the assumption of point-like source and neglecting wave optics effects (see also [10, 12, 13]. Thus, a large portion of PBH parameter space that was previously thought disfavored is now open again.

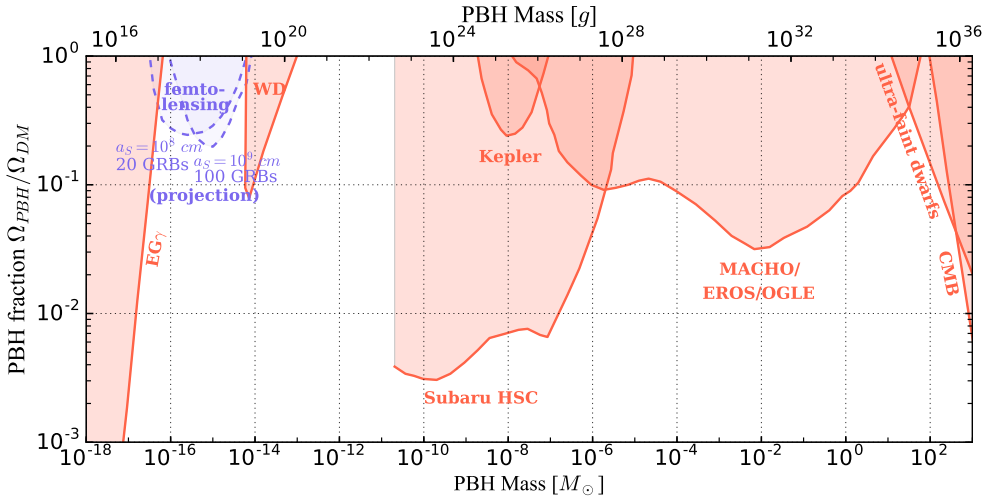

Figure 4: Current constraints on primordial black holes (red) [14] compared to potential future limits from femtolensing of GRBs (blue). Note that the assumed source diameters 10^8–10^9 cm are highly optimistic. See text and ref. [7] for a more detailed discussion.

It may still be possible to derive limits such limits in the future, but only if significantly more GRBs with well-determined redshifts are observed, and if the diameter of these sources is at the lower end of current estimates (10^9 cm). As the variability of a source is a good proxy for its size, this suggests focusing on the shortest GRBs. In fig. 4 we compare possible future femtolensing limits on PBHs (blue) together to currently established limits using other methods (red).

4. LIGO / VIRGO: Modified Binary Inspirals from Dark Forces

At the dawn of gravitational wave astronomy, it is natural to ask how observations of binary neutron star inspirals can contribute to the hunt for physics beyond the Standard Model. One proposal that has been put forward is to search for deviations from the gravitational wave forms predicted by general relativity (GR). Such deviations could be caused by new long-range forces acting between the neutron stars, and since new long-range forces coupling to Standard Model particles are tightly constrained, this idea is most interesting in the context of self-interacting DM. In fact, neutron stars are expected to contain a certain amount of DM, accumulated throughout their lifetime. However, we now argue (based on ref. [15]) that this population is never sufficient to have an observable impact on neutron star inspirals.

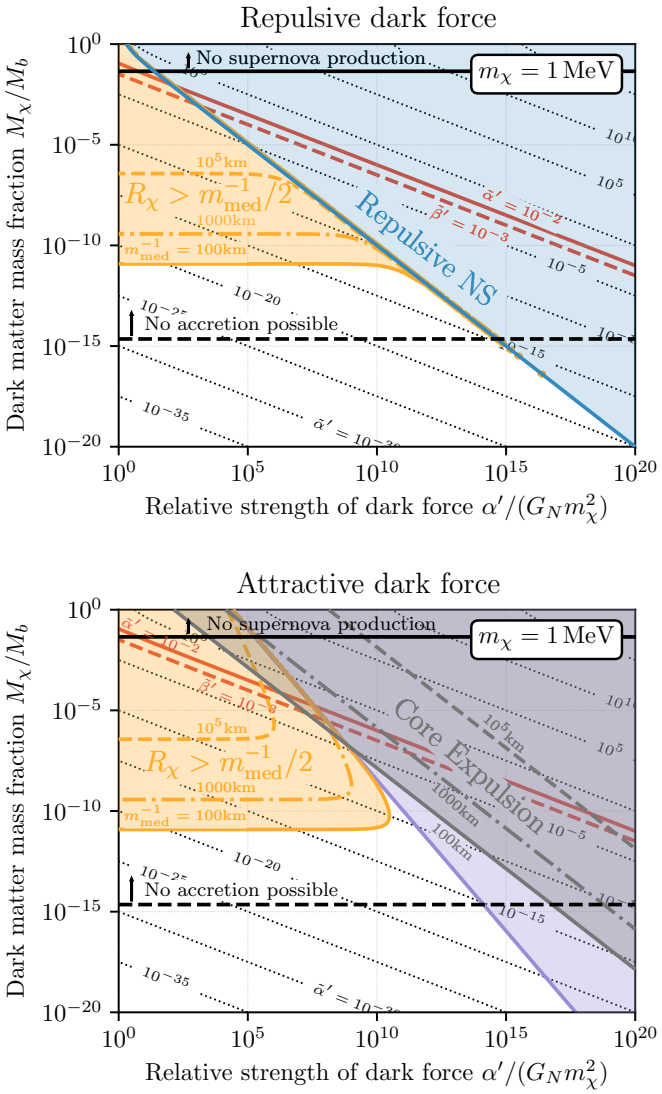

Figure 5: Constraints on repulsive *(top)* and attractive *(bottom)* long-range dark sector forces. See text and ref. [15] for details.

This is illustrated in more detail in fig. 5. For repulsive dark forces (top panel), an important constraint arises from the fact that, beyond a certain DM content, the neutron star will not be able to capture any more DM particles (light blue region). This constraint becomes important whenever the DM-to-baryon mass fraction M_χ/M_b or the strength of the dark force α' is large. For large DM content, the DM distribution will moreover extend beyond the neutron star radius, allowing outlying particles to be stripped away efficiently, which significantly reduces their effect on the inspiral (yellow region). Both constraints combined make it highly unlike that a dark force signal will be observed in LIGO. (Dotted black contours show the magnitude of the dark force effect compared to GR, and the red solid and red dashed lines show the estimated sensitivity to the direct effect of the dark force and to the effect of dark gauge boson radiation, respectively.) In fact, the parameter region accessible by LIGO is far above the maximum amount of DM a neutron star can capture

based on its geometric cross section (black dashed line). More exotic production mechanisms such as DM production in the supernova that produced the neutron star could in principle lead to a much larger DM mass fraction, but this region is disfavored by other constraints.

For attractive forces (bottom panel), many of the constraints are the same as for repulsive force. What is new is the constraint from black hole formation for too large and compact DM distributions (purple) and the constraint from core expulsion (gray). The latter constraint arises because a strong attractive force implies that the mutual attraction of the two dark cores will expel them from their host neutron stars long before the merger.

We note that a small parameter window may be open at DM masses larger than $m_\chi = 1$ MeV (the choice made in fig. 5). At $m_\chi \gg$ MeV, the yellow exclusion region disappears. However, an observable signal would still require an exotic DM production mechanism such as the formation of compact primordial DM objects that act as seeds for star formation and make up a significant (per cent level) mass fraction of at least some neutron stars.

References

[1] V. Springel et al., *The Aquarius Project: the subhalos of galactic halos*, *Mon. Not. Roy. Astron. Soc.* **391** (2008) 1685 [0809.0898].

[2] M. Buschmann, J. Kopp, B. R. Safdi and C.-L. Wu, *Stellar Wakes from Dark Matter Subhalos*, 1711.03554.

[3] H. C. Plummer, *On the problem of distribution in globular star clusters*, *Mon. Not. Roy. Astron. Soc.* **71** (1911) 460.

[4] R. H. Brandenberger, N. Kaiser and N. Turok, *Dissipationless Clustering of Neutrinos Around a Cosmic String Loop*, *Phys. Rev.* **D36** (1987) 2242.

[5] A. Gould, *Femto microlensing of gamma-ray bursters*, *Submitted to: Astrophys. J. Lett.* (1991) .

[6] A. Barnacka, J. F. Glicenstein and R. Moderski, *New constraints on primordial black holes abundance from femtolensing of gamma-ray bursts*, *Phys. Rev.* **D86** (2012) 043001 [1204.2056].

[7] A. Katz, J. Kopp, S. Sibiryakov and W. Xue, *Femtolensing by Dark Matter Revisited*, *Submitted to: JCAP* (2018) [1807.11495].

[8] T. T. Nakamura and S. Deguchi, *Wave Optics in Gravitational Lensing*, *Progress of Theoretical Physics Supplement* **133** (1999) 137.

[9] M. Bartelmann, *Gravitational Lensing*, *Class. Quant. Grav.* **27** (2010) 233001 [1010.3829].

[10] A. Barnacka and A. Loeb, *A size-duration trend for gamma-ray burst progenitors*, *Astrophys. J.* **794** (2014) L8 [1409.1232].

[11] V. Z. Golkhou, N. R. Butler and O. M. Littlejohns, *The Energy-Dependence of GRB Minimum Variability Timescales*, *Astrophys. J.* **811** (2015) 93 [1501.05948].

[12] P. Pani and A. Loeb, *Exclusion of the remaining mass window for primordial black holes as the dominant constituent of dark matter*, 1401.3025.

[13] S. Davidson and T. Schwetz, *Rotating Drops of Axion Dark Matter*, 1603.04249.

[14] K. Inomata et al., *Double inflation as a single origin of primordial black holes for all dark matter and LIGO observations*, *Phys. Rev.* **D97** (2018) 043514 [1711.06129].

[15] J. Kopp, R. Laha, T. Opferkuch and W. Shepherd, *Cuckoo's eggs in neutron stars: can LIGO hear chirps from the dark sector?*, *JHEP* **11** (2018) 096 [1807.02527].